[4]Bilanin, A. J., Teske, M. E., and Hirsh, J. E., "Neutral Atmospheric Effects on the Dissipation of Aircraft Vortex Wakes," *AIAA Journal*, Vol. 16, No. 9, 1978, pp. 956–961.

[5]Kopp, F., "Doppler Lidar Investigation of Wake Vortex Transport Between Closely Spaced Parallel Runways," *AIAA Journal*, Vol. 32, No. 4, 1994, pp. 805–810.

[6]Corjon, A., and Poinsot, T., "A Model to Define Aircraft Separations Due to Wake Vortex Encounter," AIAA Paper 95-1776, June 1995.

[7]Crow, S. C., and Bate, E. R., "Lifespan of Trailing Vortices in a Turbulent Atmosphere," *Journal of Aircraft*, Vol. 13, No. 7, 1976, pp. 476–484.

[8]Liu, H.-T., "Effects of Ambient Turbulence on the Decay of a Trailing Vortex Wake," *Journal of Aircraft*, Vol. 29, No. 1, 1992, pp. 255–263.

[9]Perry, R. B., Hinton, D. A., and Stuever, R. A., "NASA Wake Vortex Research for Aircraft Spacing," AIAA Paper 97-0057, Jan. 1997.

Low-Reynolds-Number Effects on Delta-Wing Aerodynamics

Lance W. Traub,* Brian Moeller,† and Othon Rediniotis‡
Texas A&M University,
College Station, Texas 77840-3141

Introduction

FLOW visualization has traditionally provided a powerful technique for both qualitative and quantitative investigations of delta-wing flows. Because low-speed water flows are conducive to flow visualization techniques, many studies have addressed low Reynolds number (*Re*) flow. Some examples are the investigations of Atta and Rockwell[1] at $Re = 5.8 \times 10^3$, Reynolds and Abtahi[2] at a *Re* between 1.9×10^4 and 6.5×10^4, Traub et al.[3] with *Re* in the neighborhood of 9×10^3, and Lowson[4] at *Re* as low as 6.6×10^3 (performed in a wind tunnel). However, accompanying pressure, force, and moment measurements have typically been performed at significantly higher *Re* because of sensitivity and accuracy limitations of typical pressure and load measurement instrumentation at low dynamic pressures. Most pressure and load measurement efforts have been performed at *Re* above 0.34×10^6.[5–7] The presence of this *Re* gap raises the question of flow sensitivity, particularly in the range from 10^4 to 10^5. How reconcilable are the two data sets, i.e., flow visualization data and pressure/load data? Do they describe the same flow patterns?

A compilation of data by Erickson,[8] taken from water and wind-tunnel tests as well as in flight, and spanning a *Re* range from 9.8×10^3 to 4.0×10^7, indicate that vortex location and breakdown are governed by an inviscid mechanism. Lowson[4] compared vortex core positions for a range of *Re* (between 6.6×10^3 and 1.6×10^6). Significant scatter existed in the data. He suggested that although the results appear to justify low *Re* studies of high *Re* delta-wing flows, care should be applied in certain areas in extrapolating from low to high *Re*. Roos and Kegelman[9] investigated the influence of sweep angle on delta-wing flows and concluded that vortex core trajectories, vortex burst locations and wing lift show no significant sensitivity to *Re* changes. However, the *Re* for their tests ranged between 0.34×10^6 and 2.0×10^6. A slight decrease of the maximum lift was observed with increasing *Re*. Exceptions to the practice of avoiding pressure and load measurements at low *Re* are the investigations of Lee et al.[10] ($Re = 2.3 \times 10^4$) and Gursul and Ho[11] (*Re* between 3×10^4 and 6×10^4). Lift data by Lee et al. indicate that the aerodynamic forces on delta wings are insensitive to *Re*. They also suggested that for sharp-edged wings the vortex breakdown location is independent of *Re*. A study has been undertaken to elucidate if the local flow features and the integrated coefficients are sensitive to low *Re* effects. Consequently, in this Note, an investigation of the effect of *Re* from 2×10^4 to 6×10^4 on delta wings is described. The study contains force balance, pressure, and hot-wire anemometer measurements, and on and off-surface flow visualization.

Experimental Equipment

The wind-tunnel models were manufactured from 1.27-mm aluminum plate and had a root chord, c, of 100 mm, giving a wing thickness-to-chord ratio of 1.27%. Two models were manufactured with leading-edge sweep angles, Λ, of 60 and 70 deg, respectively. The wing's leading and trailing edges were square edged. The 60-deg sweep delta was pressure tapped, with a row of 14 tappings spaced 2 mm apart located at 60% of the wing root chord (Fig. 1). An Air Neotronics autozeroing digital manometer was used to measure the pressure. This manometer can resolve pressures down to 0.1 Pa. The manometer was sampled 500 times using a 16-bit A/D board and then averaged.

The wind-tunnel tests were undertaken in a 1×1-ft low-turbulence wind tunnel. The maximum blockage for the two wings based on the projected frontal area was 3.9 and 2.7% for the Λ = 60- and 70-deg wings, respectively. The results that are presented do not include blockage or upwash corrections to avoid potentially contaminating the data. The omission of corrections (whose correct application for wings with vortical flow, particularly in flows involving vortex breakdown is uncertain) is also justifiable as the level of blockage is low. A SETRA force balance was used to measure lift. The balance has a resolution of 0.01 g.

Water-tunnel tests were undertaken in a 2×3-ft tunnel. Wing's, geometrically similar to the wind-tunnel models were manufactured for water-tunnel flow visualization, with a root chord of 200 mm. The chord of the water-tunnel models was selected to ensure that upwash effects should be equivalent for both test facilities. Measurements were also taken over the wing using a TSI 1051-2 hot-wire Anemometer system. Data

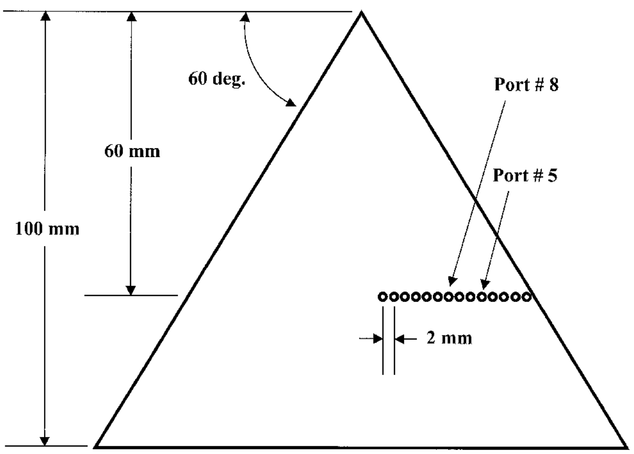

Fig. 1 Model pressure tapping details.

Received Nov. 23, 1997; revision received March 31, 1998; accepted for publication March 31, 1998.

*Graduate Student, Aerospace Engineering Department. Associate Member AIAA.

†Graduate Student, Aerospace Engineering Department. Student Member AIAA.

‡Assistant Professor, Aerospace Engineering Department. Member AIAA.

from the hot wire was analyzed using a HP 3563A spectrum analyzer, with the data presented representing 50 averaged power spectrums.

Results and Discussion

Figure 2 presents lift coefficient as a function of angle of attack, α. Included in Fig. 2 are results from the study of Wentz and Kohlman.[5] Wentz and Kohlman's results are often regarded as "baseline" and feature wings with symmetrical edges. Figure 2 shows that *Re* in the range presented have a moderate effect on the lift coefficient. Increasing *Re* is seen to result in an increase in lift for a given angle of attack. This effect is most noticeable around maximum lift, $C_{L\max}$. The low *Re* of the present tests also affect the angle of attack at which the $C_{L\max}$ occurs, with maximum lift occurring at approximately 3–4 deg higher α than in the results of Wentz and Kohlman. To see the effect of surface roughness, 100 grit was applied to the surface of the 70-deg sweep wing. As may be seen in Fig. 2b, in the tested *Re* range, the effect of roughness was marginal. Hummel[12] has shown that the boundary-layer state, although affecting the localized flow properties of the wing, has a small effect on the integrated coefficients.

Figure 3 shows the spanwise pressure distribution over the 60-deg wing, with spanwise tappings located at 60% of the root chord, as a fraction of the local semispan, *y*/*s*. It is apparent that there are marked differences between the distributions at $Re = 2 \times 10^4$, and $Re = 4 \times 10^4$ and 6×10^4. The two higher *Re* show a more pronounced suction peak and display a possible secondary separation vortex for α = 10 deg. $Re = 2 \times 10^4$ shows a suction peak further inboard than for the other two cases, with a distribution outboard of the suction peak similar to that seen in separated flow, i.e., relatively flat. At α = 30 deg the effect of vortex breakdown is seen to be one of increasing the width of the suction peak. Notice that the suction peaks migrate inboard at the higher α for $Re = 4 \times 10^4$ and 6×10^4, whereas the peak moves outboard for $Re = 2 \times 10^4$.

Figure 4a shows the vortex burst trajectories for the 60- and 70-deg delta wings. An analytic prediction of the burst trajectories is also included in the figure.[13] For the 60-deg wing, initially increasing the *Re* from 2×10^4 is seen to move the burst location upstream. Lambourne and Bryer[14] noted similar trends. The differences between the trajectories are seen to reduce as breakdown approaches the apex. Notice that $C_{L\max}$ of the 60-deg wing is reached (Fig. 2) with vortex breakdown located at approximately 17% of the wing root chord from the apex. For Λ = 70 deg, significant *Re* effects on the vortex burst location are not readily apparent (Fig. 4a).

Figures 4b and 4c show the vertical and spanwise location of the vortex cores for the two wings at α = 17 deg as a fraction of the wingspan, *b*. The data show that the effect of *Re* on the vertical position of the vortex is marginal for both Λ = 60 and 70 deg. The values also show agreement with those correlated by Lowson.[4] The lateral location of the vor-

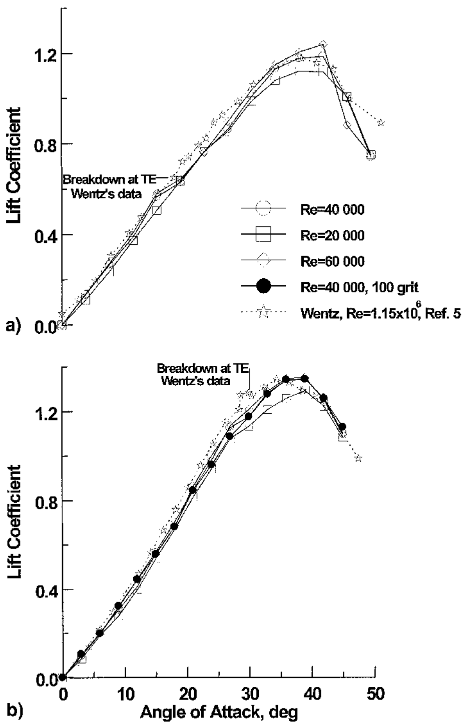

Fig. 2 Effect of *Re* on lift coefficient. Λ = a) 60 and b) 70 deg.

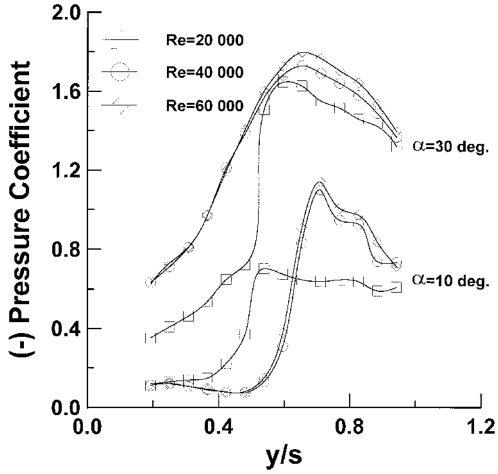

Fig. 3 Effect of *Re* on spanwise pressure distribution of Λ = 60-deg delta wing. Tappings located at 60% of wing root chord.

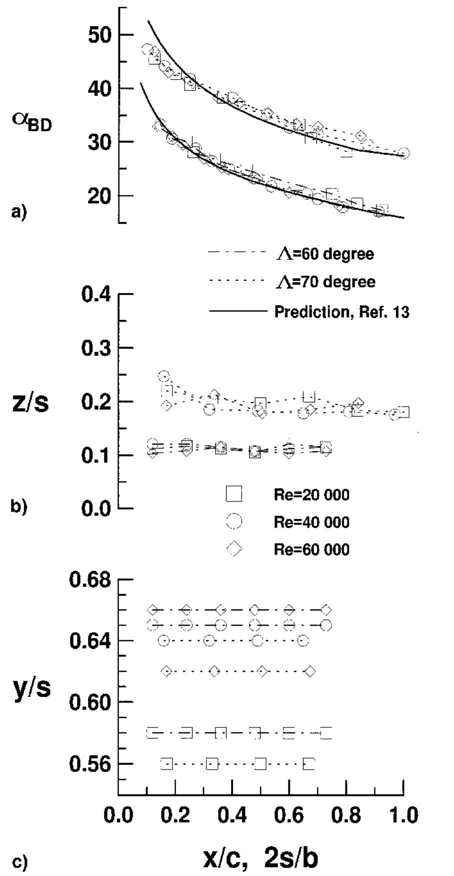

Fig. 4 Effect of *Re* on vortex trajectories for Λ = 60- and 70-deg wings: a) vortex breakdown (BD) trajectories; b) vertical vortex location, α = 17 deg; and c) spanwise vortex location, α = 17 deg.

tices is, however, seen to be sensitive to *Re* (as may also be seen in Fig. 3), with a distinct outboard migration evident for $Re = 4 \times 10^4$ and 6×10^4 compared with $Re = 2 \times 10^4$ at the same α, for both leading-edge sweep angles.

Figures 5a–5c shows surface flow visualization, representing the limiting streamlines over the 60-deg wing at $\alpha = 17$ deg. A mixture of titanium dioxide suspended in kerosene and linseed oil was used. Figure 5 shows that the flow outboard of the secondary separation line at $Re = 2 \times 10^4$ reveals large areas of semistagnant flow, resembling a three-dimensional separation bubble that correlates with the form of the pressure distribution noted in Fig. 3. The outboard migration of the vortex cores for $Re = 4 \times 10^4$ and 6×10^4, compared with $Re = 2 \times 10^4$, in Fig. 4c, is also associated with an outboard movement of the secondary separation line as shown in Fig. 5. An outboard movement of the secondary separation line is usually identified with transition of the crossflow boundary layer from laminar to turbulent. In the present study this is clearly not the mechanism responsible as the flow remains laminar, and it further suggests that an increase in *Re* from 2×10^4 to 4×10^4 is accompanied by a fundamental change in the vortex flowfield. Similar flowfield characteristics were present over the 70-deg wing (not shown). At higher *Re* a tertiary separation line is visible near the wing apex, indicating the presence of a secondary and possible tertiary vortex.

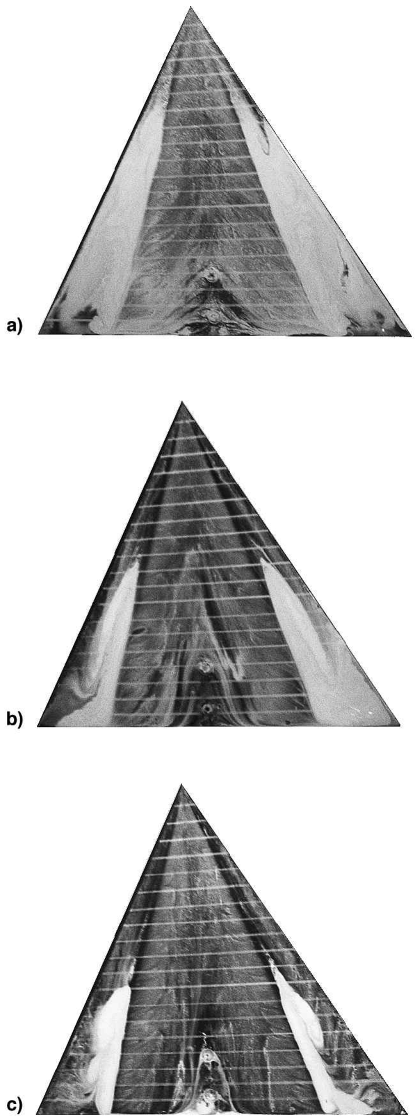

Fig. 5 Effect of *Re* on limiting streamline pattern over $\Lambda = 60$-deg wing, $\alpha = 17$ deg. Re = a) 2×10^4, b) 4×10^4, and c) 6×10^4.

The preceding data suggest that there is a transition in the flowfield between $Re = 2 \times 10^4$ and $Re = 4 \times 10^4$. To determine the nature of the transition, and if the transition is marked by a Hopf-type bifurcation (indicating a critical value of *Re* at which the nature of the flowfield changes), further tests were undertaken, mostly in this *Re* range.

To establish if any of the flow regimes were marked by surface pressure/velocity fluctuations, measurements using a hot-wire anemometer were undertaken. The hot wire was orientated such that it was perpendicular to the freestream and located at $z/s = 0.06$ above ports 5 and 8 (Fig. 1). As may be seen in Fig. 6 (which was acquired above port 5, but is also representative of that seen at port 8), the data do not show the existence of any periodic or coherent flow structures. This was also found to be the case for *Re* between those presented. Hubner and Komerath[15] noted the existence of nearly periodic velocity fluctuations, associated with streakline oscillations. These structures were not observed at the α and *Re* where the present hot-wire data were acquired.[15]

Figure 7 shows the effect of increasing *Re* on the average spanwise location of the vortices. It is clear that the outboard migration of the vortices for both the $\Lambda = 60$- and 70-deg delta wings is a gradual and relatively linear motion, and is not marked by any sudden translation.

Re effects on the pressure measured at ports 5 and 8 (Fig. 1), on the $\Lambda = 60$-deg wing, are depicted in Fig. 8. The reduction in the pressure coefficient at port 8 with increasing *Re* is associated with the spanwise movement of the vortex cores, such that port 8 is no longer directly under the core (for $Re > 2 \times 10^4$). For port 5, which as shown in Fig. 3 is located close to the location of the minimum pressure coefficient for all of the core locations in this study, increasing the *Re* is generally associated with a gradual decrease in the pressure coefficient.

To determine if the flowfield showed any significant hysteresis effects, the $\Lambda = 60$-deg wing was set at $\alpha = 30$ deg, with the *Re* being increased and then subsequently decreased. The surface pressure was recorded at port 5. As may be seen in

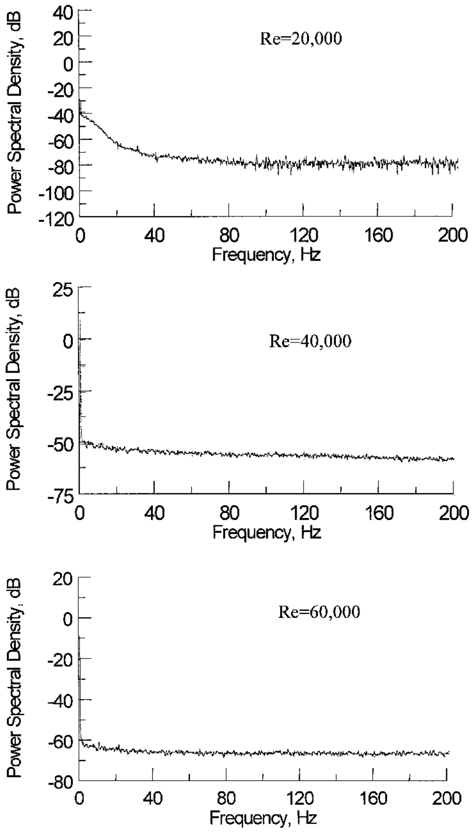

Fig. 6 Effect of *Re* on power spectrum, port 5, $z/s = 0.06$.

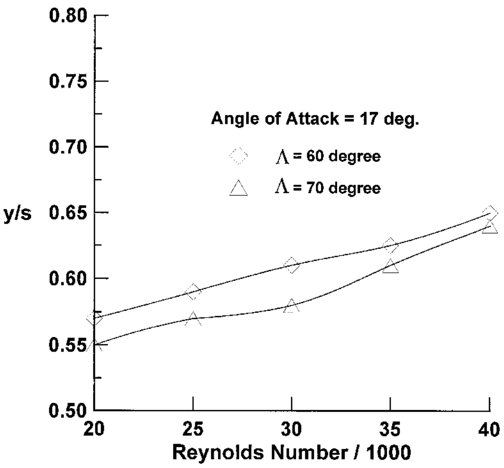

Fig. 7 Effect of *Re* on vortex spanwise trajectory.

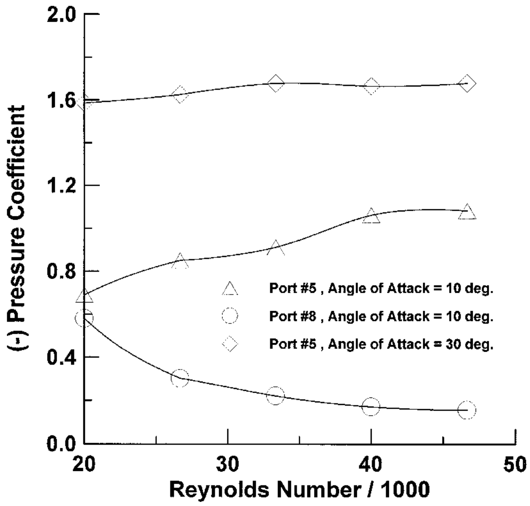

Fig. 8 Effect of *Re* on surface pressure coefficient, Λ = 60 deg.

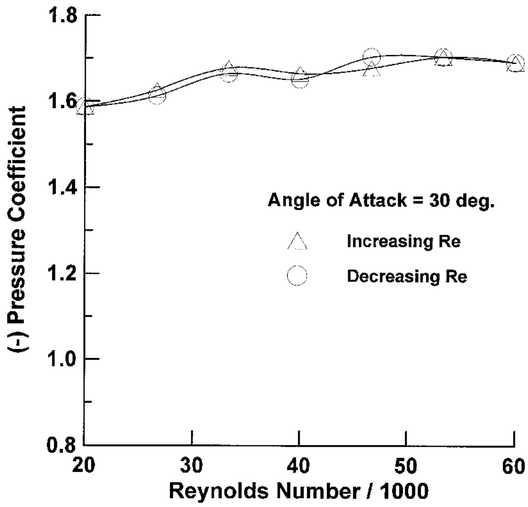

Fig. 9 Hysteresis effect of increasing and decreasing *Re* on surface pressure.

Fig. 9 the pressure distribution showed no evidence of any significant hysteresis effects.

The results suggest that the change of the flow characteristics occurring between a *Re* of 2×10^4 to 4×10^4 is marked by a gradual change of the flow properties, with the existence of a critical *Re* not being apparent. The variation of surface pressure and vortex spanwise location with *Re* is smooth, with the flow showing no periodic flow structures close to the wing surface.

Concluding Remarks

An experimental study was undertaken to determine the aerodynamic characteristics of a 60- and 70-deg delta wing at low *Re*. Tests were undertaken with the *Re* ranging from 2×10^4 to 6×10^4. The data show that *Re* effects on lift are marginal, however, the maximum lift coefficient occurs at a higher angle of attack than at high *Re*. There does, however, appear to be a change in the characteristics of the vortical flowfield when the *Re* is decreased from 4×10^4 to 2×10^4. At $Re = 2 \times 10^4$, the vortices and secondary separation line are further inboard than at the higher *Re*, and for the 60-deg delta, vortex breakdown at a given angle of attack is delayed. For the 60-deg delta, the form of the spanwise pressure distribution at $Re = 2 \times 10^4$ differs from that seen at a *Re* of 4×10^4 and 6×10^4. The variation of the surface pressure and vortex trajectory with *Re* was gradual, with no marked transition within the *Re* range of study.

Acknowledgments

The authors thank Murray Tobak, whose suggestions for further research greatly enhanced the completeness of this study. Thanks are also extended to Sam Galls for his assistance with the data presentation.

References

[1]Atta, R., and Rockwell, D., "Leading-Edge Vortices Due to Low Reynolds Number Flow Past a Pitching Delta Wing," *AIAA Journal*, Vol. 28, No. 10, 1990, pp. 995–1004.

[2]Reynolds, G. A., and Abtahi, A. A., "Instabilities in Leading-Edge Vortex Development," AIAA Paper 87-424, Jan. 1987.

[3]Traub, L. W., Rediniotis, O. K., Klute, S. M., and Telionis D. P., "Instabilities of Vortex Breakdown; Their Structure and Growth," AIAA Paper 95-2308, June 1995.

[4]Lowson, M. V., "Visualization Measurements of Vortex Flows," *Journal of Aircraft*, Vol. 28, No. 5, 1991, pp. 320–327.

[5]Wentz, W. H., and Kohlman D. L., "Vortex Breakdown on Slender Sharp Edged Wings," *Journal of Aircraft*, Vol. 8, No. 3, 1971, pp. 156–161.

[6]Kegelman, J. T., and Roos, F. W., "Effects of Leading Edge Shape and Vortex Burst on the Flowfield of a 70-Degree-Sweep Delta Wing," AIAA Paper 89-0086, Jan. 1989.

[7]Bragg, M. B., and Soltani, M. R., "An Experimental Study of the Effect of Asymmetrical Vortex Bursting on a Pitching Delta Wing," AIAA Paper 88-4334, Aug. 1988.

[8]Erickson, G. E., "Water-Tunnel Studies of Leading-Edge Vortices," *Journal of Aircraft*, Vol. 19, No. 6, 1982, pp. 442–448.

[9]Roos, F., and Kegelman, J. T., "An Experimental Investigation of Sweep-Angle Influence on Delta-Wing Flows," AIAA Paper 90-0383, Jan. 1990.

[10]Lee, M., Shih, C., and Ho, C.-M., "Response of a Delta Wing in Steady and Unsteady Flows," *ASME 1987 Fluids Engineering Conference*, Vol. 52, American Society of Mechanical Engineers, New York, 1987, pp. 19–24.

[11]Gursul, H. L., and Ho, C. M., "Vorticity Dynamics of 2-D and 3-D Wings in Unsteady Free Stream," AIAA Paper 91-0010, Jan. 1991.

[12]Hummel, D., "On the Vortex Formation over a Slender Wing at Large Angles of Incidence," *High Angle of Attack Aerodynamics*, AGARD, CP-247, Jan. 1979.

[13]Traub, L. W., "Prediction of Vortex Breakdown and Longitudinal Characteristics of Swept Slender Planforms," *Journal of Aircraft*, Vol. 34, No. 3, 1997, pp. 353–359.

[14]Lambourne, N. C., and Bryer, D. W., "The Bursting of Leading Edge Vortices—Some Observations and Discussion of the Phenomenon," Aeronautical Research Council, R&M 3282, London, April 1961.

[15]Hubner, J. P., and Komerath, N. M., "Modification of Spectral Characteristics in a Vortex Flow Field," AIAA Paper 95-1795, June 1995.